

Ni d -band self-energy beyond the low-density limit

Ansgar Liebsch

Institut für Festkörperforschung, Kernforschungsanlage Jülich, 517 Jülich, West Germany

(Received 15 July 1980)

Previous calculations of the Ni d -band self-energy within the low-density approximation are improved by considering correlations due to both hole-hole and electron-hole interactions. It is shown that these additional processes tend to reduce the satellite binding energy and enhance the narrowing of the d band. The exchange splitting is decreased only by a small amount from the value obtained in the low-density limit. The new results are in good agreement with experimental photoemission spectra.

I. INTRODUCTION

In a previous paper,¹ it has been shown that the main features of experimental Ni d -band photoemission spectra can be semiquantitatively understood by considering explicitly the self-energy corrections to the valence bands due to correlations between $3d$ electrons. As a result of these corrections, the width² of the Ni d band is about 25% smaller than predicted by band theory³ while the exchange splitting⁴ is about half as large as the band value. Furthermore, the self-energy corrections explain the existence of the satellite structure⁵ below the d band as well as the relatively large intrinsic width⁶ of individual band states in angle-resolved energy distributions.

In order to interpret the photoemission spectra, it is assumed that they can be represented (apart from one-electron matrix element effects) by the spectral function of the created hole state⁷

$$A_{\nu\mu\sigma}(\omega, \vec{k}) = \frac{1}{\pi} \text{Im} \left(\frac{1}{\omega - \epsilon_{\nu\sigma}(\vec{k}) - \Sigma_{\nu\sigma}(\omega, \vec{k})} \right)_{\nu\mu}, \quad (1)$$

where $\epsilon_{\nu\sigma}(\vec{k})$ represents a diagonal matrix containing the band energies $\epsilon_{\nu\sigma}(\vec{k})$ and $\Sigma_{\nu\sigma}(\omega, \vec{k}) = \Sigma_{\nu\mu\sigma}(\omega, \vec{k})$ denotes the self-energy matrix. The self-energy is evaluated by using the degenerate Hubbard model⁸ to describe interactions between d electrons at the same site and by making the so-called low-density approximation (LDA).⁹ The attractive feature of this approximation is that it leads to an exact expression for the self-energy in the limit in which the number of holes in the d band is small and the interaction between d electrons is short ranged.¹⁰ These conditions are thought to be reasonably well satisfied in the case of Ni.¹¹

As pointed out above, this model, though physically rather simple, permits indeed an adequate overall interpretation of the main features of observed photoemission spectra. Nevertheless, in one particular aspect, the results predicted by the LDA cannot be reconciled with experiment:

If the strength of the intra-atomic Coulomb interaction is chosen so that it gives the measured band narrowing, the binding energy of the satellite turns out to be several eV too large.^{1,12,13} On the other hand, if the Coulomb integral is adjusted to give the observed satellite position, the band narrowing is too small. The purpose of the present paper is to show that this discrepancy is in fact related to the inadequacy of the low-density limit and that it can be removed by including processes in the evaluation of the self-energy which are of higher than first order in the number of unfilled d states.

Physically, this effect may be understood as follows: In the LDA, the self-energy represents an exact summation of processes to all orders in the repulsion of two holes below E_F . Thus, its energy dependence is governed by the bare two-hole spectral distribution, i.e., essentially by the self-convolution of the occupied portion of the bare density of states. Poles in the self-energy due to the existence of two-hole bound states appear, therefore, below the two-hole continuum which is roughly twice as wide as the d band. In going beyond the LDA it is necessary to include processes involving the excitation of electrons from states below E_F into the unoccupied part of the d band. The effect of such processes may be viewed as a renormalization of the hole states through which their spectral density is strongly skewed towards E_F and effectively narrowed. As a result of this renormalization, the two-hole distribution is also skewed towards E_F and therefore leads to self-energy poles at lower binding energies. Thus, the neglect of electron-hole interactions in the LDA tends to overestimate the binding energy of the two-hole bound state.

In the case of a ferromagnetic system, the renormalization described above is particularly strong because of the possible resonant scattering between electrons and holes of opposite spin. We show below that the explicit summation of hole-hole and electron-hole ladders then gives an ex-

pression for the self-energy which is equivalent to that derived by Hertz and Edwards¹⁴ in their treatment of multiple hole-magnon interactions. One may conclude from these considerations, therefore, that the low-density approximation is quite capable of describing the overall features of the photoemission spectra, but that it is necessary to go beyond the LDA in order to discuss details such as the precise location of the satellite or the correct amount of band narrowing. The exchange splitting, on the other hand, turns out to be relatively little effected by processes involving electron-hole interactions. Its small measured value seems to be mainly determined by correlations due to the repulsion of hole pairs which form the basis of the self-energy in the low-density limit.

II. THE LOW-DENSITY LIMIT

Before considering the influence of electron-hole interactions on the self-energy, it is useful to review briefly the results obtained within the LDA. It is assumed here that the main energy dependence of the self-energy of Ni is related to the presence of unoccupied d states and that all scattering processes involving s electrons may be neglected. The rather good agreement between band calculations and angle-resolved photoemission spectra in the case of Cu (Ref. 15) supports this approximation.

In the low-density limit, the self-energy is given in terms of the t matrix involving the Coulomb interaction and the two-hole propagator. Treglia *et al.*¹⁶ have recently examined the momentum dependence on this propagator in the single-band case and found that it has negligible influence on the structure of the self-energy. We assume this to be true also for a d band and replace the full propagator by its momentum average (this corresponds to the "local" term in Ref. 16). As a result, the t matrix is also \vec{k} independent. This approximation leads to a considerable simplification since it can be shown that the self-energy expressed in an angular momentum representation is diagonal and independent of \vec{k} . Thus, one finds

$$\Sigma_{\nu\mu\sigma}(\omega, \vec{k}) = \sum_{n=1}^5 a_{\nu n\sigma}^*(\vec{k}) a_{\mu n\sigma}(\vec{k}) \Sigma_{n\sigma}(\omega),$$

where n denotes the d -orbital index and the $a_{\nu n\sigma}^*(\vec{k})$ represent expansion coefficients of Bloch states in terms of atomic orbitals.

The self-energy components $\Sigma_{n\sigma}(\omega)$ may be written as

$$\Sigma_{n\uparrow}(\omega) = - \sum_{m=1}^5 n_{m\uparrow} t_{nmnm}(\omega), \quad (2)$$

$$\Sigma_{n\uparrow}(\omega) = - \sum_{m=1}^5 n_{m\uparrow} [t_{nmnm}(\omega) - t_{nmnm}(\omega)].$$

In principle, these expressions should contain energy integrals extending over the unoccupied part of the minority-spin density of states. However, since this energy interval is very small in the case of Ni, the integral may be replaced by the corresponding hole occupation numbers $n_{m\uparrow}$. The t matrix is defined as

$$t_{m_1 \dots m_4}(\omega) = \left(\frac{1}{1 + UG^{(2)}(\omega)} \right)_{m_1 \dots m_4} \quad (3)$$

with

$$U_{m_1 \dots m_4} = \langle \phi_{m_1}(\vec{r}_1) \phi_{m_2}(\vec{r}_2) | U_{sc} | \phi_{m_3}(\vec{r}_1) \phi_{m_4}(\vec{r}_2) \rangle \quad (4)$$

and

$$G^{(2)}(\omega) = \int d\epsilon_1 \int d\epsilon_2 \frac{\rho(\epsilon_1) \rho(\epsilon_2) f(\epsilon_1) f(\epsilon_2)}{\omega - \epsilon_1 - \epsilon_2 - i\delta}. \quad (5)$$

U_{sc} represents the screened Coulomb interaction between d electrons and the $\phi_m(\vec{r})$ are products of radial functions and real spherical harmonics.

In Eq. (5), the dependence of the two-hole propagator $G^{(2)}(\omega)$ on orbital and spin indices is, for simplicity, neglected. (As a result, the t matrix is also spin independent.) More accurately, $G^{(2)}(\omega)$ should contain the partial wave projections of the ferromagnetic density of states. However, because Eq. (5) involves a double integral, the components of $G^{(2)}(\omega)$ are rather insensitive to the detailed shape of the density-of-state projections. We therefore may replace these projections by a weighted average over spin and orbital indices which we denote by $\rho(\epsilon)$. The quantity $f(\epsilon)$ is the usual Fermi function. It should be noted, though, that this approximation is not necessary for the evaluation of Eq. (2). The main motivation for using it in the present derivation is the fact that the self-energy then assumes a particularly transparent form.

If $G^{(2)}(\omega)$ is independent of orbital and spin indices, Eq. (2) can be greatly simplified by diagonalizing the Coulomb matrix (the pairs m_1, m_2 and m_3, m_4 are treated as matrix indices):

$$\Sigma_{i\sigma}(\omega) = - \sum_{\alpha=1}^5 \sum_{j=1}^2 A_{ij\alpha}^{\sigma} n_{j\uparrow} t_{\alpha}(\omega), \quad (6)$$

where $i, j \equiv t_{2g}, e_g$, and the components of the t matrix are defined as

$$t_{\alpha}(\omega) = \frac{u_{\alpha}}{1 + u_{\alpha} G^{(2)}(\omega)}. \quad (7)$$

The u_α represent the eigenvalues of the Coulomb matrix. They are linear combinations of the usual Slater integrals¹⁷ for *d* orbitals:

$$u_\alpha = F^{(0)} + a_\alpha F^{(2)} + b_\alpha F^{(4)} \quad (8)$$

and correspond to the term energies of the d^8 multiplet. The numerical values of the coefficients a_α , b_α , and $A_{ij\alpha}^\sigma$ which appear in Eqs. (6) and (8) are given in Table I.

Equation (6) shows that each multiplet term introduces its own energy-dependent structure into the self-energy of a $3d$ hole. Thus, in the low-density limit, the photoemission spectrum shows atomiclike as well as bandlike behavior.¹ Since for Ni the intra-atomic interactions and the bandwidth are of comparable size,¹⁸ the atomic multiplet is only partly visible and the individual band states are shifted towards E_F as well as broadened, thereby effectively causing an overall narrowing of the *d* band.

According to Eq. (7), the binding energies of the satellite features are solely determined by the size of the interaction parameters u_α and by the shape of the bare two-hole distribution defined in Eq. (5). The approximations which have been made in the derivation of Eq. (6) do not significantly effect this characteristic behavior. On the one hand, the neglect of the \vec{k} dependence in Eqs. (5) to (7) amounts to the omission of the finite hopping probability of two holes bound to the same site. Satellites that are split off below the two-hole continuum thus appear in the above treatment as sharp spectral features whereas in principle they should show a small intrinsic width. On the other hand, the orbital dependence of $G^{(2)}(\omega)$ should produce a weak coupling between the terms of the d^8 multiplet whereas above they lead to separate contributions to the self-energy.

It is evident, therefore, that the overestimation of the satellite binding energy in Refs.

TABLE I. Coefficients a_α and b_α , Eq. (8), and $A_{ij\alpha}^\sigma$, Eq. (6). $A_{ij\alpha}^\sigma = 2A_{ij\alpha}^\sigma$ for $\alpha = \text{triplet state}$, zero otherwise.

α	1S	1G	3P	1D	3F
a_α	$\frac{2}{7}$	$\frac{4}{49}$	$\frac{1}{7}$	$-\frac{3}{49}$	$-\frac{8}{49}$
b_α	$\frac{2}{7}$	$\frac{1}{441}$	$-\frac{4}{21}$	$\frac{4}{49}$	$-\frac{1}{49}$
$A_{11\alpha}^\dagger$	$\frac{1}{5}$	$\frac{38}{35}$	$\frac{1}{5}$	$\frac{5}{7}$	$\frac{4}{5}$
$A_{12\alpha}^\dagger$	0	$\frac{5}{7}$	$\frac{2}{5}$	$\frac{2}{7}$	$\frac{3}{5}$
$A_{21\alpha}^\dagger$	0	$\frac{15}{14}$	$\frac{3}{5}$	$\frac{3}{7}$	$\frac{9}{10}$
$A_{22\alpha}^\dagger$	$\frac{1}{5}$	$\frac{51}{70}$	0	$\frac{4}{7}$	$\frac{1}{2}$

1 and 12 is a direct consequence of the low-density approximation itself. By tuning the interaction energies, one could make the satellite positions agree with experiment. Within the LDA, however, this would reduce the amount of band narrowing far below the observed value. In the following section, it will be shown that it is possible to remove this discrepancy by going beyond the low-density limit.

Since the screened Coulomb interaction is not well known, the $F^{(n)}$ are in our calculations treated as parameters. Their actual values, however, in particular those of $F^{(2)}$ and $F^{(4)}$, can be determined reasonably well experimentally from core-valence-valence Auger spectra.¹⁸ In the case in which the interatomic interactions between valence *d* electrons are negligible compared with the intra-atomic ones, the Auger spectrum for a filled band is given¹⁹ (aside from matrix element effects) by a formula that is closely related to the *t* matrix in Eq. (3):

$$A(\omega) = \frac{1}{\pi} \text{Im Tr} \left(\frac{G^{(2)}(\omega)}{1 + UG^{(2)}(\omega)} \right), \quad (9)$$

where Tr denotes the trace of a matrix. The dependence of $G^{(2)}(\omega)$ on \vec{k} and orbital indices is again omitted. Applying the same diagonalization of the Coulomb matrix as above, this expression may be simplified to

$$A(\omega) = \frac{1}{\pi} \text{Im} \sum_{\alpha=1}^5 m_\alpha \frac{G^{(2)}(\omega)}{1 + u_\alpha G^{(2)}(\omega)}, \quad (10)$$

where the m_α are multiplicities of the five terms of the d^8 multiplet.

Thus, in the limit of weak intra-atomic Coulomb interactions, the Auger spectrum is given by the self-convolution of the density of states, while, for sufficiently strong interactions, $A(\omega)$ is determined by the atomic d^8 multiplet with little influence due to the remainder of the solid. At intermediate values of the u_α , $A(\omega)$ consists of a complicated superposition of five terms. Each of these carries weight in the energy range of the two-hole continuum and also at the energy of a two-hole bound state if u_α exceeds a critical value roughly the size of the bandwidth.²⁰

III. BEYOND THE LOW-DENSITY LIMIT

We consider now the influence of additional contributions to the self-energy due to electron-hole interactions in order to show that they tend to reduce the satellite binding energies from the values obtained within the low-density limit. Since

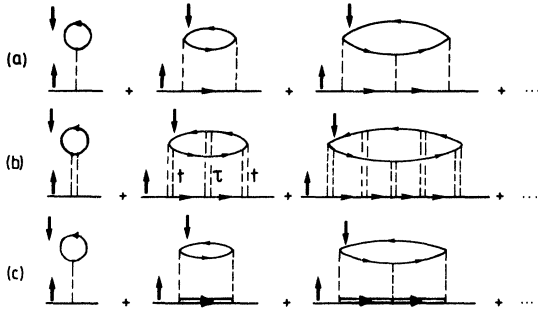


FIG. 1. Self-energy contributions for strongly ferromagnetic system (a) due to repeated scattering of hole pairs (low-density limit) and (b) due to hole-hole and electron-hole interactions. (c) Approximate form of (b) for low-density system where electron-hole interactions are absorbed into renormalized hole propagator (solid double line).

we are only interested in the qualitative consequences of these interactions, we limit this discussion to the case of a strongly ferromagnetic s band. However, for reasons that will become more evident later on, we retain the \vec{k} dependence of the self-energy. Instead of Eqs. (5)–(7), the LDA expressions then have the following form [see Fig. 1(a)]:

$$\Sigma_{\uparrow}(\omega, \vec{k}) = -n_{\uparrow} t(\omega, \vec{k}), \quad (11)$$

$$t(\omega, \vec{k}) = \frac{U}{1 + U G^{(2)}(\omega, \vec{k})}, \quad (12)$$

$$\begin{aligned} \Sigma_{\uparrow}^{(2)}(\omega, \vec{k}) = & \int \frac{d\omega_1}{2\pi i} \cdots \int \frac{d\omega_3}{2\pi i} \sum_{\vec{k}_1, \dots, \vec{k}_3} G_{\uparrow}(\omega_1, \vec{k}_1) \tau(\omega - \omega_1, \vec{k} - \vec{k}_1) G_{\uparrow}^{\dagger}(\omega_2, \vec{k}_2) t(\omega + \omega_2, \vec{k} + \vec{k}_2) G_{\uparrow}^{\dagger}(\omega_3, \vec{k}_3) \\ & \times t(\omega + \omega_3, \vec{k} + \vec{k}_2) G_{\uparrow}(\omega + \omega_2 - \omega_1, \vec{k} + \vec{k}_2 - \vec{k}_1) \\ & \times G_{\uparrow}(\omega + \omega_3 - \omega_1, \vec{k} + \vec{k}_3 - \vec{k}_1). \end{aligned} \quad (16)$$

Since we are still concerned with a low-density system, we may simplify the above equation by utilizing the following approximate equality [see also Eq. (11)]:

$$\sum_{\vec{q}} \int \frac{d\epsilon}{2\pi i} G_{\uparrow}^{\dagger}(\epsilon, \vec{q}) g(\omega + \epsilon, \vec{k} + \vec{q}) = -n_{\downarrow} g(\omega, \vec{k} + \vec{k}_0), \quad (17)$$

where g is assumed to have no poles in the lower half-plane. Since this condition is satisfied by the quantities G_{\uparrow} and t , Eq. (16) reduces to

$$\Sigma_{\uparrow}^{(2)}(\omega, \vec{k}) = n_{\downarrow}^2 t^2(\omega, \vec{k}) s(\omega, \vec{k}), \quad (18)$$

where

$$\begin{aligned} G^{(2)}(\omega, \vec{k}) = & \sum_{\vec{q}} \int \frac{d\epsilon}{2\pi i} G_{\uparrow}(\epsilon, \vec{q}) \\ & \times G_{\uparrow}(\omega - \epsilon, \vec{k} + \vec{k}_0 - \vec{q}). \end{aligned} \quad (13)$$

Here, we have assumed that the hole states are distributed over an energy range that is small compared with the bandwidth and that they are located in a small region of \vec{k} space near the point \vec{k}_0 . The corresponding self-energy for minority spins vanishes, since the majority band is filled.

The first few self-energy diagrams that contain both hole-hole and electron-hole interactions are shown in Fig. 1(b). The dashed double lines represent hole-hole ladders, as defined in Eqs. (12) and (13), or the corresponding electron-hole ladders which are given by

$$\tau(\omega, \vec{k}) = \frac{U}{1 + U\chi(\omega, \vec{k})}, \quad (14)$$

$$\chi(\omega, \vec{k}) = \sum_{\vec{q}} \int \frac{d\epsilon}{2\pi i} G_{\uparrow}^{\dagger}(\epsilon, \vec{q}) G_{\uparrow}(\omega + \epsilon, \vec{k} + \vec{q}). \quad (15)$$

Since the majority states are fully occupied, the propagator of an electron above the Fermi energy is denoted for clarity by G_{\uparrow}^{\dagger} . Accordingly, propagators without superscript refer to hole states below E_F .

Using this notation, the second diagram in Fig. 1(b) for example, gives the following self-energy expression:

$$\begin{aligned} s(\omega, \vec{k}) = & \sum_{\vec{q}} \int \frac{d\epsilon}{2\pi i} G_{\uparrow}(\epsilon, \vec{q}) G_{\uparrow}^{\dagger}(\omega - \epsilon, \vec{k} + \vec{k}_0 - \vec{q}) \\ & \times \tau(\omega - \epsilon, \vec{k} - \vec{q}). \end{aligned} \quad (19)$$

It is easily shown that higher-order processes involving alternating hole-hole and electron-hole ladders can be simplified in a similar manner. Together with the first-order expression, Eq. (11), they form the following series:

$$\begin{aligned} \Sigma_{\uparrow}(\omega, \vec{k}) = & \Sigma_{\uparrow}^{(1)}(\omega, \vec{k}) + \Sigma_{\uparrow}^{(2)}(\omega, \vec{k}) + \cdots \\ = & -n_{\downarrow} \frac{t(\omega, \vec{k})}{1 + n_{\downarrow} t(\omega, \vec{k}) s(\omega, \vec{k})} \\ = & -n_{\downarrow} \bar{t}(\omega, \vec{k}). \end{aligned} \quad (20)$$

Using Eq. (12), the renormalized t matrix defined by the last equality may be written as

$$\bar{t}(\omega, \vec{k}) = \frac{U}{1 + U\bar{G}^{(2)}(\omega, \vec{k})}, \quad (21)$$

with

$$\begin{aligned} \bar{G}^{(2)}(\omega, \vec{k}) &= G^{(2)}(\omega, \vec{k}) + n_{\uparrow} S(\omega, \vec{k}) \\ &= \sum_{\vec{q}} \int \frac{d\epsilon}{2\pi i} G_{\uparrow}(\epsilon, \vec{q}) \bar{G}_{\uparrow}(\omega - \epsilon, \vec{k} - \vec{q}) \end{aligned} \quad (22)$$

and

$$\begin{aligned} \bar{G}_{\uparrow}(\omega, \vec{k}) &= G_{\uparrow}(\omega, \vec{k} + \vec{k}_0) [1 + n_{\uparrow} G_{\uparrow}(\omega, \vec{k} + \vec{k}_0) \tau(\omega, \vec{k})], \\ &\approx \frac{G_{\uparrow}(\omega, \vec{k} + \vec{k}_0)}{1 + U\chi(\omega, \vec{k})}, \end{aligned} \quad (23a)$$

$$\approx \frac{-1}{n_{\uparrow}} \frac{\chi(\omega, \vec{k})}{1 + U\chi(\omega, \vec{k})}, \quad (23b)$$

$$\equiv \frac{-1}{n_{\uparrow}} \chi_{\text{RPA}}(\omega, \vec{k}). \quad (24)$$

In the derivation of Eqs. (23), we have applied Eq. (17) in order to obtain an approximate form for $\chi(\omega, \vec{k})$ for a low-density system:

$$\chi(\omega, \vec{k}) \approx -n_{\uparrow} G_{\uparrow}(\omega, \vec{k} + \vec{k}_0). \quad (25)$$

Equations (23) and (24) demonstrate that, in a low-density system, the summation of both hole-hole and electron-hole ladders amounts to a renormalization of the up-spin hole propagator in which the original propagator is effectively substituted by the RPA susceptibility, divided by the number of unfilled states in the minority band. The resulting self-energy

$$\Sigma_{\uparrow}(\omega, \vec{k}) = -n_{\uparrow} \frac{U}{1 + U\bar{G}^{(2)}(\omega, \vec{k})}, \quad (26)$$

$$\bar{G}^{(2)}(\omega, \vec{k}) = \sum_{\vec{q}} \int \frac{d\epsilon}{2\pi i} G_{\uparrow}(\epsilon, \vec{q}) \frac{-1}{n_{\uparrow}} \chi_{\text{RPA}}(\omega - \epsilon, \vec{k} - \vec{q}), \quad (27)$$

is of the same form as that obtained in the low-density limit, Eq. (11). The t matrix and the bare two-hole propagator are, however, replaced by the corresponding renormalized quantities as defined in Eqs. (21) and (22). Hence, the self-energy may again be represented by a series of ladder diagrams of the type shown in Fig. 1(c). The dashed lines indicate the bare Coulomb interaction as in Fig. 1(a), while the solid double lines denote the renormalized majority-spin hole propagator defined in Eqs. (23) and (24).

It should be noted that the above derivation is nearly exact; the only approximate step involves

the application of Eq. (17) which utilizes the fact that the minority holes are distributed over a small energy region and a small part of the Brillouin zone. This approximation is made, moreover, only at some stages in the evaluation of the diagrammatic series. In particular, it is avoided in the intermediate summation of electron-hole ladders which ultimately lead to the appearance of the RPA susceptibility in the renormalized propagator, Eq. (27).

The main feature of the above result which we want to draw attention to is the fact that the spectral weight of the renormalized hole propagator, Eq. (23), is concentrated at considerably lower energies than that of the bare propagator. The reason for this is the dominance of the magnon pole and of low-lying single-particle excitations in χ_{RPA} , Eq. (24). Cooke *et al.*²¹ have recently calculated in a detailed study the dynamic susceptibility for Ni within the RPA by including the energy and wave-vector dependence of the matrix elements. Their results demonstrate that most of the spectral weight of χ_{RPA} is concentrated at energies below 0.8 eV. The spectral distribution of the two-hole propagator, Eq. (27), is therefore strongly skewed towards smaller binding energies. This shift of weight implies, in turn, that the self-energy, Eq. (26), has, for a given value of U , a pole at lower energies than the original self-energy in the low-density limit, Eq. (11). Qualitatively, we can conclude from the above derivation that the LDA, in which interactions between bare holes are included, tends to overestimate the binding energy of the two-hole bound state.

The diagrams shown in Fig. 1(b) include electron-hole ladders only for states of opposite spin. In the general case of a strongly ferromagnetic d band, one should in principle consider also the other type of electron-hole ladders in which both particles carry minority spins. In a low-density system, it can be shown that this leads to a renormalization of the minority-hole propagator in analogy to that obtained above for majority states, Eq. (23). While this renormalization for parallel spins is not as pronounced as for antiparallel spins, it also tends to reduce the spectral width of the effective two-hole distribution. Thus, for a real system such as Ni, this effect should further lower the satellite binding energies from the values obtained within the LDA.

It should be pointed out here that self-energy expressions similar to that in Eq. (26) have been previously derived by Roth²² using an equation-of-motion scheme, and by Hertz and Edwards,¹⁴ who consider self-energy contributions due to multiple hole-magnon interactions. In the latter

case, the following result is obtained instead of Eq. (26)²³:

$$\Sigma_{\uparrow}(\omega, \vec{k}) = -n_{\uparrow} \frac{U}{1 + \Sigma'_{\text{RPA}}(\omega, \vec{k})/n_{\uparrow}U}, \quad (28)$$

where

$$\Sigma_{\text{RPA}}(\omega, \vec{k}) = -U^2 \sum_{\vec{q}} \int \frac{d\epsilon}{2\pi i} G_{\uparrow}(\epsilon, \vec{q}) \chi_{\text{RPA}}(\omega - \epsilon, \vec{k} - \vec{q}) \quad (29)$$

represents the RPA self-energy which accounts for hole-magnon scattering to lowest order. The prime in Eq. (28) indicates that the RPA susceptibility in (29) is to be replaced by the exact susceptibility in order to make the entire theory self-consistent.

As can be seen from Eq. (27), $\Sigma_{\text{RPA}}(\omega, \vec{k})$ differs from our renormalized two-hole propagator only by a constant factor:

$$\Sigma_{\text{RPA}}(\omega, \vec{k}) = n_{\uparrow} U^2 \bar{G}^{(2)}(\omega, \vec{k}). \quad (30)$$

Hence, apart from the additional self-consistency requirement in Eq. (28), the self-energies in Eqs. (26) and (28) are identical. This result might appear surprising since the two expressions are derived using rather different mathematical procedures. Physically, on the other hand, both approaches are equivalent since multiple hole-magnon interactions amount to repeated scattering events of hole-hole and electron-hole pairs of opposite spin.

In order to illustrate more quantitatively the influence of the renormalization of the hole propagator due to electron-hole interactions, we have performed model calculations for typical two-hole spectral distributions. Since we are primarily interested in the energy region in the vicinity of the satellite, we neglect the \vec{k} dependence of $\bar{G}^{(2)}(\omega, \vec{k})$ and replace it by its momentum average. Equations (26) and (27) then simplify to

$$\Sigma_{\uparrow}(\omega) = -n_{\uparrow} \frac{U}{1 + U\bar{G}^{(2)}(\omega)}, \quad (31)$$

$$\bar{G}^{(2)}(\omega) = \int \frac{d\epsilon}{2\pi i} G_{\uparrow}(\epsilon) \frac{-1}{n_{\uparrow}} \chi_{\text{RPA}}(\omega - \epsilon), \quad (32)$$

where $\chi_{\text{RPA}}(\omega)$ represents the \vec{k} -averaged susceptibility. [Note that this average does not imply a momentum average of the Pauli susceptibility, Eq. (15). The latter would be a much more severe approximation since it would not give the correct spin-flip excitation spectrum.]

Figure 2(a) shows schematically the spectral distribution of two bare holes (dashed line) and the renormalized spectrum (solid line) which is

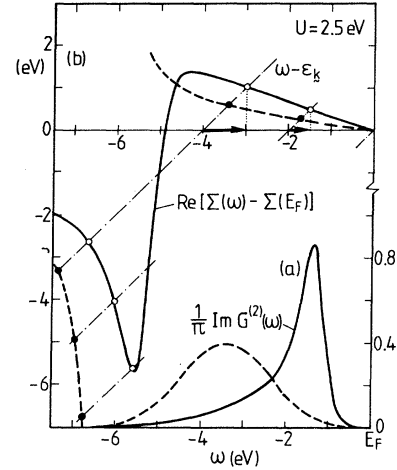


FIG. 2. (a) Schematic spectral distribution of renormalized (solid line) and bare (dashed line) two-hole propagator. (b) Real part of corresponding self-energies for $U=2.5$ eV. The intersections with the lines $\omega - \epsilon_{\vec{k}}$ specify the shifted band energies and the positions of the two-hole bound states.

skewed towards E_F . The weight under both curves is taken to be unity. The renormalized spectrum is chosen in accordance with Eq. (32), i.e., it corresponds to the convolution of the density of states with a function that is strongly peaked at low energies in order to represent qualitatively the shape of $\chi_{\text{RPA}}(\omega)$. The real parts of the corresponding self-energies are plotted in (b) for $U=2.5$ eV. The number of holes n_{\uparrow} in Eq. (31) is chosen appropriate to Ni (≈ 0.53). Since the intersections or $\text{Re } \Sigma(\omega)$ with the line $\omega - \epsilon_{\vec{k}}$ lead to maxima in the spectral function, they define the shifted quasiparticle energies and the satellites. [The intersections near -5 eV produce only weak background contributions in the spectral function since the imaginary part of $\Sigma(\omega)$ is very large in this energy region. See, for example, Fig. 1 of Ref. 1.]

These results demonstrate that the renormalization of the two-hole spectrum has two effects:

(i) the satellites are moved to lower binding energies and (ii) the shift of band states towards E_F is enhanced. The reason for the latter feature is that the real part of the self-energy becomes steeper just below E_F as the spectral weight of $\bar{G}^{(2)}(\omega)$ is concentrated at lower binding energies. Thus, the correct amount of band narrowing is now obtained for a much smaller value of U (≈ 2.5 eV) than previously¹ for the bare two-hole spectrum ($U \approx 5$ eV).

This smaller value of U is identical to the one used recently by Davis and Feldkamp²⁴ in their evaluation of the Ni self-energy. These authors achieve a satisfactory fit of the band narrowing

and the satellite binding energy by numerically solving the Hubbard model for a finite number of atoms and assuming the hole in the *d* band to be stationary. Since in this approach all types of excitation processes are included, the *U* parameter should, as it does, correspond more closely to that obtained for the renormalized two-hole spectrum than to the value of *U* used in the LDA.

Typical hole spectral distributions for band states at -4 , -3 , and -2 eV are shown in Fig. 3. These results are based on the renormalized two-hole distribution of Fig. 2. The crosses indicate the weight of each spectrum within the band region (approximately -5 eV $\leq \omega \leq E_F$). The total weight including the satellite is unity.) These curves illustrate that the overall narrowing of the *d* band in angle-integrated spectra has three sources: Band states near the bottom of the *d* band (i) are shifted more strongly towards E_F , (ii) they contribute considerably more weight to the satellite, and (iii) they exhibit a larger intrinsic broadening²⁵ than states in the upper part of the band.

Since $\text{Re } \Sigma(\omega)$ increases roughly linearly with ω (see Fig. 2), the shift of individual band states is also proportional to their binding energy, the constant of proportionality being approximately 0.8, as found experimentally. The calculated lifetime broadening of states near the bottom of the band agrees well with the measured values (≈ 1.2 eV), but is somewhat too small at lower binding energies. Since the imaginary part of the self-energy is largely determined by $\text{Im } \bar{G}^{(2)}(\omega)$ [see Eq. (31)], this suggests that the renormalized two-hole spectrum shown in Fig. 2 contains apparently too little weight in the energy region just

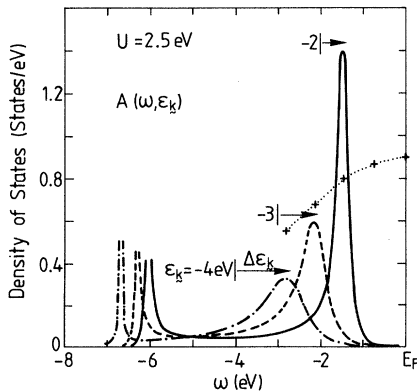


FIG. 3. Spectral distributions of several band states obtained from renormalized self-energy shown in Fig. 2. The crosses indicate the weight under each peak within the band region.

below E_F . Because of the strong energy dependence of the real and imaginary parts of the self-energy, the maxima of the hole distributions in the band region in Fig. 3 do not coincide exactly with the corresponding intersections of $\omega - \epsilon_{\vec{k}}$ and $\text{Re } \Sigma(\omega)$ in Fig. 2. Thus, the measured peak positions in angle resolved spectra lie always at slightly lower binding energies than the true quasiparticle states, the discrepancy being largest near the bottom of the *d* band.

The above results indicate that electron-hole scattering processes not included in the low-density approximation have a pronounced influence on the satellite binding energies and on the shifts of band states. In remarkable contrast to this behavior, the exchange splitting turns out to be relatively little effected if one goes beyond the LDA. For t_{2g} and e_g states, the splitting is given by the expression

$$\Delta_i = \Sigma_{i\downarrow}(E_F) - \Sigma_{i\uparrow}(E_F), \quad i = t_{2g}, e_g. \quad (33)$$

In principle, the self-energy of a strongly ferromagnetic *d* band in the presence of hole-hole and electron-hole interactions could give rise to a complicated mixing of multiplet terms in Eq. (6) as a result of the dependence of the renormalized two-hole propagator on \vec{k} and on band and spin indices. Since a full calculation of this effect goes beyond the scope of the present work, it will be assumed for the purpose of the following qualitative arguments that the major effect of electron-hole scattering events on Δ_i is to alter the value of the real part of $\bar{G}^{(2)}(E_F)$. (The imaginary part vanishes at E_F .) Thus we continue to use Eqs. (6) and (7) to evaluate Δ_i but the two-hole propagator is now modified as indicated schematically in Fig. 2.

Since the renormalized spectral distribution of $\bar{G}^{(2)}(\omega)$ is narrower and closer to E_F than the bare spectrum, $\bar{G}^{(2)}(E_F)$ must be larger than $G^{(2)}(E_F)$. For the particular example shown in Fig. 2, an increase from approximately 0.3 to 0.6 eV⁻¹ as a result of the renormalization is found. The magnitude of $G^{(2)}(E_F)$ might therefore be used as a measure for the importance of electron-hole interactions. In order to illustrate the effect of this renormalization on the exchange splitting, $\Delta_{t_{2g}}$ and Δ_{e_g} are shown in Fig. 4 as a function of $G^{(2)}(E_F)$ for typical values of *U* and $F^{(2)}$.^{26,27} In all cases, a decrease of Δ_i is found for increasing $G^{(2)}(E_F)$. However, this decrease tends to be rather small, of the order of 0.1 eV. Qualitatively it can be said that the smallness of the observed exchange splitting is primarily determined by two-hole correlations and that electron-hole processes appear to cause an additional reduction by a relatively small amount.

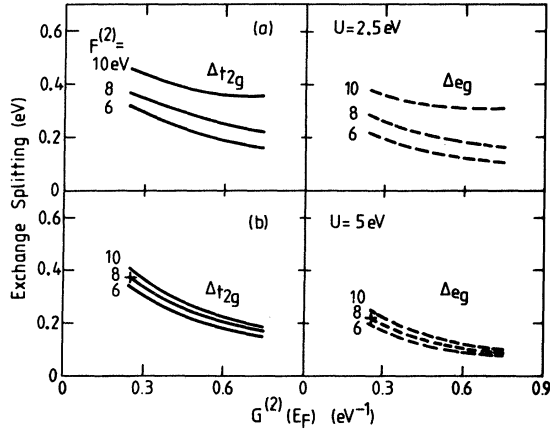


FIG. 4. Exchange splittings $\Delta_{t_{2g}}$ and Δ_{e_g} as function of $G^{(2)}(E_F)$ for typical values of U and $F^{(2)}$. $F^{(4)} = 0.6F^{(2)}$. The crosses indicate the splittings obtained in Ref. 1. Larger values of $G^{(2)}(E_F)$ imply increasing importance of electron-hole interactions.

The Coulomb and exchange integrals are taken as parameters in the above calculations. It is therefore important to establish that the derived values of $\Delta_{t_{2g}}$ and Δ_{e_g} do not depend sensitively on the particular $F^{(n)}$ that are used. To some extent this point is already evident from the results shown in Fig. 4. In order to illustrate more systematically the relationship between the exchange splittings and the $F^{(n)}$, $\Delta_{t_{2g}}$ and Δ_{e_g} are shown in Fig. 5 as function of U for various values of $F^{(2)}$ and $G^{(2)}(E_F)$. Except when U is small and $F^{(2)}$ is at the same time large, the dependence of Δ_i on U is remarkably weak. The origin of this insensitivity is the well known fact that the Coulomb and exchange contributions to Δ_i tend to partly compensate one another.²⁹

Expanding the u_α in Eqs. (6) to (8) about U , the exchange splittings may be approximately written as

$$\begin{aligned} \Delta_{t_{2g}} &\simeq n_{t_{2g}\uparrow}(Uc + 2J_1c^2) + n_{e_g\downarrow}2J_3c^2 \\ \Delta_{e_g} &\simeq n_{e_g\uparrow}(Uc + J_2c^2) + n_{t_{2g}\downarrow}3J_3c^2, \end{aligned} \quad (34)$$

where

$$c^{-1} = 1 + UG^{(2)}(E_F) \quad (35)$$

and the J_i denote various exchange integrals between t_{2g} and e_g orbitals.²⁶ With increasing U , the term Uc increases monotonically towards a finite value given by the inverse of $G^{(2)}(E_F)$, whereas all other terms containing the J_i decrease to zero. Thus, for a wide range of $F^{(n)}$, the t_{2g} and e_g exchange splittings lie between 0.2 and 0.4 eV in the case of the bare two-hole spectrum [Fig. 5(a)], while the corresponding splittings for the renormalized spectrum are roughly

0.1 eV smaller [Fig. 5(b)].

Because of the theoretical limitations of the above model calculations, it is not possible at the moment to make a more accurate prediction of the exchange splittings. Qualitatively, however, both the low-density limit and its extension give estimates that lie clearly far below the band theoretical value of $\approx 0.65 \text{ eV}$.³ Moreover, as Figs. 4 and 5 demonstrate, the e_g exchange splitting is consistently smaller than the t_{2g} splitting because of the anisotropy of the spin density³⁰ [see Eq. (34)]. Recent angle resolved photoemission measurements in the vicinity of the L_3 and X_2 critical points confirm this result, giving splittings of about 0.3 eV [Refs. 4(a), (b)] and 0.17 eV [Ref. 4(c)], respectively.

IV. CONCLUSION

Previous calculations of the Ni d -band self-energy within the low-density limit suggested that hole-hole correlations provide a useful basis to understand the discrepancies between measured photoemission spectra and one-electron band theory. The aim of the present work has been to go beyond the low-density approximation in order to consider in addition the influence of electron-hole interactions. The results indicate that these processes are non-negligible for Ni. Certain quantitative aspects of the self-energy obtained within the LDA are significantly improved. Specifically, the binding energy of the satellite below the d band is reduced and the amount of band narrowing is enhanced. Both features can be made to agree with experiment for

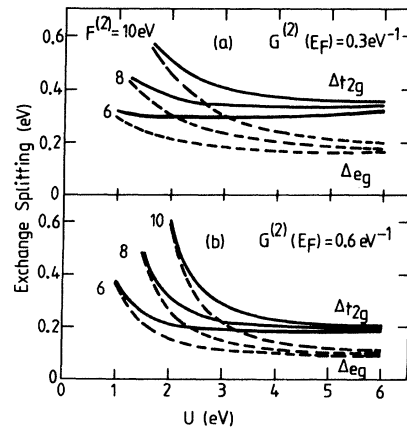


FIG. 5. Exchange splittings $\Delta_{t_{2g}}$ and Δ_{e_g} as function of $G^{(2)}(E_F)$ for typical values $F^{(2)}$. $F^{(4)}_{e_g} = 0.6F^{(2)}$. $G^{(2)}(E_F)$ is approximately appropriate (a) to bare two-hole spectrum (low-density limit) and (b) to renormalized two-hole spectrum (beyond low-density limit).

the same intra-atomic Coulomb energy (≈ 2.5 eV). The small size of the exchange splittings (0.2 to 0.4 eV), on the other hand, seems to be mainly the result of hole-hole correlations. Electron-hole interactions lead to an additional lowering of $\Delta_{t_{2g}}$ and Δ_{e_g} by only about 0.1 eV.

The effect of electron-hole interactions may be understood as a renormalization of the hole propagators so that the effective two-hole spectral distribution is considerably narrower and concentrated at lower energies than the bare two-hole spectrum. This viewpoint suggests an interesting interpretation of the Hubbard expression of the self-energy at low densities.⁸ Since it differs from Eq. (31) only in that $\bar{G}^{(2)}(\omega)$ is replaced by $G(\omega)$, the Hubbard solution corresponds to an approximation in which the effective two-hole spectral density is taken to be the bare one-hole distribution, i.e., the density of states.

The above results must be regarded as qualitative in nature since the full degeneracy of the *d* band is not included³¹ and since only certain kinds of scattering processes involving alternating hole-hole and electron-hole ladders for opposite spins are considered. For a strongly ferromagnetic system, these are likely to represent the most important types of interactions. As we have shown, the self-energy derived for these processes is equivalent to that obtained for multiple hole-magnon interactions.¹⁴ Furthermore, the self-energy should in principle be corrected for the amount of correlation already contained in the band calculation. This correction would primarily effect the band narrowing and the satellite position. The exchange splitting is less sensitive to such modifications since it depends on

the band information only in a rather indirect manner [see Eqs. (34), (35), and also Fig. 4].

All of the recent theoretical calculations of the Ni *d*-band self-energy^{1, 12-14, 24} suggest that the characteristic features observed in Ni photoemission spectra are caused by (i) the strength of the intra-atomic Coulomb energy relative to the bandwidth and (ii) the presence of unoccupied states in the *d* band. In the case of Cu, therefore, none of these features are observable since the *d* band is filled. In the case of Fe and Co,³² on the other hand, the discrepancies between the band calculation and experimental spectra are smaller than for Ni because of the smaller size of U/W .

Tersoff *et al.*³³ have shown that the origin of the core-level satellites in Ni can be understood in a similar way as the *d*-band satellite. In both cases, the emission of the photoelectron is accompanied by the excitation of a *d* electron into the unfilled portion of the *d* band. Since the interaction between the originally created core or *d* hole with this additional band hole is sufficiently strong, a discrete excited state is observed at higher binding energies. If this mechanism is correct, the satellite intensity should diminish as the Ni *d*-band occupancy is increased. Such an experiment has recently been performed³⁴ by alloying Ni with Th which tends to donate electrons to the Ni host. With increasing Th concentration, the XPS spectra show gradually decreasing weight at the satellites of both the *d* band and the Ni core levels.

ACKNOWLEDGMENT

I wish to thank Professor D. Rainer for fruitful discussions.

¹A. Liebsch, Phys. Rev. Lett. **43**, 1431 (1979).

²S. Hüfner, G. K. Wertheim, N. V. Smith, and M. M. Traum, Solid State Commun. **11**, 323 (1972).

³C. S. Wang and J. Callaway, Phys. Rev. B **15**, 298 (1977).

⁴(a) D. E. Eastman, F. J. Himpsel, and J. A. Knapp, Phys. Rev. Lett. **40**, 1514 (1978); (b) E. Dietz, U. Gerhardt, and C. Maetz, Phys. Rev. Lett. **40**, 892 (1978); U. Gerhardt, C. Maetz, A. Schütz, and E. Dietz, J. Magn. Magn. Mater. **15-18**, 1141 (1980); (c) P. Heilmann and H. Neddermeyer, J. Magn. Magn. Mater. **15-18**, 1143 (1980).

⁵C. Guillot, Y. Ballu, J. Paigné, J. Lecante, K. P. Jain, P. Thiry, R. Pinchaux, Y. Pétrouff, and L. M. Falicov, Phys. Rev. Lett. **39**, 1632 (1977).

⁶W. Eberhardt and E. W. Plummer, Phys. Rev. B **21**, 3245 (1980).

⁷L. Hedin and S. Lundqvist, Solid State Phys. **23**, 1 (1969).

⁸J. Hubbard, Proc. R. Soc. London, Ser. A **277**, 237 (1964).

⁹J. Kanamori, Prog. Theor. Phys. **30**, 235 (1963).

¹⁰V. M. Galitskii, Zh. Eksp. Teor. Fiz. **34**, 14 (1958) [Sov. Phys.—JETP **7**, 104 (1958)].

¹¹N. D. Lang and H. Ehrenreich, Phys. Rev. **168**, 605 (1968).

¹²D. Penn, Phys. Rev. Lett. **42**, 921 (1979).

¹³G. Treglia, F. Ducastelle, and D. Spanjaard, Phys. Rev. B **21**, 3729 (1980).

¹⁴J. A. Hertz and D. M. Edwards, J. Phys. F **3**, 2174 (1973).

¹⁵P. Thiry, D. Chandesris, J. Lecante, C. Guillot, R. Pinchaux, and Y. Pétrouff, unpublished.

¹⁶G. Treglia, F. Ducastelle, and D. Spanjaard, J. Phys. (Paris) **41**, 281 (1980).

¹⁷J. C. Slater, *Quantum Theory of Atomic Structure*, Vol. I (McGraw-Hill, New York, 1960), Chap. 13.

¹⁸E. Antonides, E. C. Janse, and G. A. Sawatzky, Phys.

- Rev. B 15, 1669 (1977); 15, 4596 (1977); E. Antonides and G. A. Sawatzky, Inst. Phys. Conf. Ser. 39, 134 (1978).
- ¹⁹G. A. Sawatzky, Phys. Rev. Lett. 39, 504 (1977); M. Cini, Solid State Commun. 24, 681 (1977).
- ²⁰A. Liebsch, unpublished.
- ²¹J. F. Cooke, J. W. Lynn, and H. L. Davis, Phys. Rev. B 21, 4118 (1980).
- ²²L. M. Roth, Phys. Rev. 186, 426 (1969).
- ²³Since in Ref. 14 electrons instead of holes are considered, some of the signs are reversed.
- ²⁴L. C. Davis and L. A. Feldkamp, Solid State Commun. 34, 141 (1980).
- ²⁵J. B. Pendry, in *Photoemission and the Electronic Properties of Surfaces*, edited by B. Feuerbacher, B. Fitton, and R. F. Willis (Wiley, New York, 1978), p. 97.
- ²⁶The parameters U and J_i are related to the Slater integrals in the following manner:
- $$U = F^{(0)} + \frac{4}{49} F^{(2)} + \frac{4}{49} F^{(4)},$$
- $$J_1 = \frac{3}{49} F^{(2)} + \frac{20}{441} F^{(4)},$$
- $$J_2 = \frac{4}{49} F^{(2)} + \frac{15}{441} F^{(4)},$$
- $$J_3 = \frac{2}{49} F^{(2)} + \frac{25}{441} F^{(4)}.$$
- ²⁷In all calculations we have used $F^{(4)} = 0.6F^{(2)}$. This relationship follows the trend observed in Auger spectra (see Ref. 18) and is also found theoretically: see R. E. Watson, Phys. Rev. 118, 1036 (1960).
- ²⁸A more complicated behavior occurs at small values of U if $F^{(2)}$ is large (see Fig. 5).
- ²⁹C. Herring, in *Magnetism*, Vol. 4, edited by G. Rado and H. Suhl (Academic, New York, 1966), Chap. 10.
- ³⁰See also, L. Hodges, H. Ehrenreich, and N. D. Lang, Phys. Rev. 152, 505 (1966); O. Gunnarsson, J. Phys. F 6, 587 (1976); E. Marschall and H. Bross, Phys. Status Solidi B 90, 241 (1978).
- ³¹The multiplet terms in Eq. (6) would, for example, be coupled due to the electron-hole interactions. The 1S peak in the hole spectral function might therefore not be as clearly separated from the other terms as in the low-density limit (see Fig. 2 of Ref. 1).
- ³²D. E. Eastman, F. J. Himpsel, and J. A. Knapp, Phys. Rev. Lett. 44, 95 (1980).
- ³³J. Tersoff, L. M. Falicov, and D. R. Penn, Solid State Commun. 32, 1045 (1979).
- ³⁴J. C. Fuggle, unpublished.